The effect of parameters of the initial data updating algorithm on the accuracy of spacecraft reentry time prediction

A.I. Nazarenko[a 1], I.V. Usovik[b],

[a]Retired Professor, Malakchitovaya str 12-1-52, 129128, Moscow, Russia.

[b]Scientific Research Institute for System Analysis, the Russian Academy of Sciences, Moscow

Abstract

The problem under consideration has drawn attention of experts in connection with the events of large-size, dangerous spacecraft reentry. Traditionally, this problem has been solved on the basis of application of the least squares technique. In so doing, the "weighing" of measurements is carried out disregarding the random atmospheric disturbances. For the example of Tiangong-1 spacecraft reentry determination, the effect of the updating algorithm parameters on the accuracy of spacecraft reentry prediction is estimated. The characteristics of accounting for atmospheric disturbances at "weighing" the measurements and the fit span value are considered as the algorithm parameters. It is shown that, when the random atmospheric disturbances are taken into account, the accuracy of results grows several times.

Keywords

Reentry, least squares technique, optimum filtration of measurements, fit span.

1. Introduction

The problem under consideration has drawn attention of experts in connection with the events of large-size, dangerous spacecraft (SC) reentry. These spacecraft include, for example, Skylab, Cosmos 954, Cosmos 1402, Salute 7–Cosmos 1686, Tiangong-1, etc. The feature of the majority of dangerous reentries is the absence of communication with spacecraft and the impossibility of controlling them. Under these conditions, the basic source of initial orbital data for solving this problem are the results of operation of Russian and American Space Surveillance Systems (SSS). The orbital data on many satellites, in the form of so-called two-line elements (TLE), are regularly and operatively updated on a website of the American SSS (the Joint Space Operations Center) [1].

The technique for solving the considered problem is based on the integration of the equations of motion with the known initial data (ID) consisting of a 6-dimensional state vector and the drag parameter estimate. Different characteristics are used as the drag parameters. The most popular of them is the value of ballistic factor (Sb) and the change of the orbital period under an effect of atmospheric drag per revolution (ΔT).

[1] *Corresponding author*
E-mail address: anazarenko32@mail.ru

The feature of the considered problem solution is the sensitivity of results to the accuracy of the initial drag characteristic. The point is that the SC lifetime is inversely proportional to the drag characteristic $t_{\text{life}} \approx C/Sb$, where C is some constant. This gives rise to the important dependence for estimating the lifetime determination errors, which are proportional to the lifetime and the errors in drag value estimates:

$$\delta t_{\text{life}} \approx \frac{\delta Sb}{Sb} \cdot t_{life} . \qquad (1)$$

Numerous investigations have shown that, in the most cases, the RMS of relative errors in determining the drag characteristics at the initial time instant and over the forecast interval are equal to 10 – 15 %. This level of errors remains unchanged within the last 30 years. As a result, the RMS of reentry time determination, in calculating the lifetime for 1 day, usually equals 2 – 3 hours. In some cases, the errors can be ever greater.

To determine (update) the initial data (ID) based on measurements, the Least Square Technique (LST) is traditionally used. This method was developed 200 years ago, when the artificial Earth satellites (AES) did not exist yet. A characteristic feature of AES motion is the essential effect of perturbing factors, the estimation of which is not susceptible to mathematical description to a required accuracy. A typical example of such kind of perturbances is the atmospheric drag, the value of which is proportional to the product of a real ballistic factor by the atmospheric density. The main difficulty in considering these factors at forecast consists in their unpredictable change in time. When using the LST, the effect of perturbing factors is revealed in the necessity of choosing the optimum, so-called measurement interval (the fit span), i.e. the time interval, over which the used measurements are located. The investigations have shown that the value of an optimum depends not only on the drag value, but also on the accuracy and quantity of measurements. As usual, this interval is determined from the experience and is set to be constant for particular types of satellites.

The fundamentals of the advanced ID updating technique based on measurements (the optimum filtering of measurements, OFM) were published almost 40 years ago [2]. This technique was updated later [3 – 5]. The characteristic feature of the developed technique was the allowance for statistical characteristics of atmospheric perturbances over the measurement-processing interval and in the motion forecasting, which leads to increasing the accuracy. The strict mathematical proof of this effect is stated in Section 9 «Comparison of accuracy parameters obtained with using various measurement-processing techniques» of monograph [5]. It is shown that the optimum filtering of measurements provides more accurate estimates as compared to the LST application with or without accounting for interfering parameters.

Favorable conditions for performing the analysis, considered in this paper, arose at the beginning of 2018, when the Inter Agency Debris Comity (IADC)

initiated the international test campaign on determining the time and place of the Tiangong-1 SC reentry. The representatives of 11 space agencies took part in this campaign. Preliminary materials of the campaign were discussed at the 4th International Space Debris Re-entry Workshop (ESA/ESOC, Darmstadt, Germany, 28 February – 1 March 2018), and the campaign results were summarized at the 36th IADC Plenary Meeting (Tsukuba, Japan, 5 – 8 June, 2018).

In the world, there exist two organizations, which have regularly and operatively published the results of determining the expected reentry time of satellites. These organizations are: the Joint Space Operations Center [1] and the Aerospace Corp.'s Center for Orbital and Reentry Debris Studies [6]. In addition, Dr. V.S. Yurasov has informally participated in this campaign ([7], the website: satmotion.ru).

Thus, the materials on determining the reentry time for the Tiangong-1 SC, listed above, occurred to be very useful for a comparative analysis of the problem solution accuracy with using different ID updating techniques.

2. Problem solution technology

Our technology of SC reentry time determination is presented schematically in fig. 1.

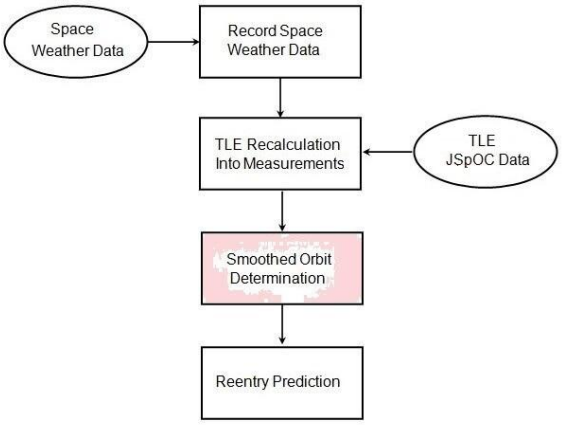

Figure 1. Calculation technology scheme

We will consider it briefly.

1. For correct solution of the stated task, it is necessary to know the data on the space weather. The values of solar activity indices $F_{10.7}$ and geomagnetic disturbance K_p (A_p) are used as input parameters in the models for atmospheric density calculation using the GOST model [8]. The celestrak.com website [9] was chosen as a source of these data.
2. The TLEs from the JSpOC website [1] were used as a source of the orbital information for calculations. These orbits were considered as measurements at updating the orbital elements and corresponding ballistic factors.
3. For each of chosen ID updating techniques, the calculation of SC reentry time and place was carried out. In the numerical integration of the equations

of motion, the instant of SC reaching the altitude of 80 km was chosen as a lifetime termination criterion.

The calculation of statistical characteristics of atmospheric perturbances at ID updating was implemented in the form of a special software module. The autocorrelation function of atmospheric perturbances was accepted to have the following form:

$$K_q(t,\tau)_0 = \begin{cases} \sigma_q^2\left(1-\dfrac{|t-\tau|}{\Delta}\right), by\ |t-\tau|<\Delta, \\ 0, by\ |t-\tau|\geq\Delta. \end{cases} \quad (2)$$

The initial data for applying this correlation function are:

ΔT – the change of the period under an effect of atmospheric drag per revolution, which is calculated on the numerical integration basis with the average ballistic factor value;

k_{atm} – RMS of random atmospheric perturbances with respect to their average value.

Δ – the interval of correlation of atmospheric perturbances.

The first two quantities are used for calculating the RMS of atmospheric drag variations by formula

$$\sigma_q = k_{atm}\cdot|\Delta T|. \quad (3)$$

The matrices of mutual correlation of errors in state vector forecasting for time instants (t_i and t_l) and ID time t_j are calculated by formula

$$M\left[\delta x(t_i)\cdot\delta x^T(t_l)\right] = K_x(t_i,t_l) = U(t_i,t_j)\cdot K_x(t_j,t_j)\cdot U(t_l,t_j)^T + Q_{il}^{(j)}, \quad (4)$$

where

$$Q_{il}^{(j)} = \int_{t_j}^{t_i}\int_{t_j}^{t_l} U(t_i,\xi)\cdot B(\xi)\cdot K_q(\xi,\eta)_0\cdot B^T(\eta)\cdot U^T(t_l,\eta)\cdot d\eta\cdot d\xi \quad (5)$$

Here $U(t_i,\xi)$ is the so-called transition matrix of dimension (6 × 6), $B(\xi)$ is the matrix of coefficients at atmospheric drag in the differential equations of disturbed motion.

In the OFM technique, the problem of estimating the state vector x (n×1) from measurements Z *(k×1)* was considered in the classical formulation. The possibility of existence of some interfering parameters q (*m×1*) was taken into consideration. In this case, the basic initial relation looks like:

$$Z = \mathrm{X}\cdot x + \mathrm{B}\cdot q + V. \quad (6)$$

Here X *(k×n)* and B (*k×m*) are known matrices, V (*k×1*) is the vector of errors in measurements, which were accepted to be equally accurate and statistically independent, i.e.

$$M(V\cdot V^T) = \sigma_z^2\cdot E. \quad (7)$$

The correlation matrix of interfering parameters $M(q\cdot q^T) = \sigma_z^2\cdot K_q$ was constructed with allowance for correlation of atmospheric perturbances and was used for "weighing" the measurements without expanding the state vector. The

effect of interfering parameters was taken into account by means of their combining with the errors of measurements $V_\Sigma = B \cdot q + V$, and then the maximum likelihood method was applied. In this case, the required estimate is expressed with using the classical formula

$$\hat{x} = \left(X^T \cdot P \cdot X\right)^{-1} \cdot X^T \cdot P \cdot Z, \tag{8}$$

where P is a square weighting matrix of dimension $k \times k$. Here k is equal to the product of a number of measurements n_z by the dimension of a unit vector of measurements.

The feature of estimate (8) lies in the fact that it is suitable for any time instants, including the forecast one. The value of interfering parameters (noises) was calculated *after* constructing the estimate (8) based on residual discrepancies (or residuals) with using the relationship of the form

$$\hat{q} = F \cdot (Z - X \cdot \hat{x}), \tag{9}$$

where F is some matrix.

The control of the ID updating algorithm parameters was carried out in the Smoothed Orbit Determination unit. At specifying $k_{atm} = 0$, matrix P becomes diagonal, and the algorithm turns into the least squares technique. Thus, the varied parameters are k_{atm} and n_z.

All calculations have been performed based on the last measurements over the time interval 2.3 days prior to reentry. The reference TLEs are presented in Table 1. It is seen from these data that there were 14 TLE sets on this interval. The average time interval between successive measurements was τ =0.16 days. When n_z measurements are used in a particular updating, the measured interval (fit span) will be $(n_z - 1) \times \tau$ days.

Table 1. Reference TLE values

1 37820U 11053A 18089.35483310 .01405725 90155-5 21632-3 0 9999
2 37820 42.7462 211.5821 0009229 349.2429 11.0621 16.32954918373600
1 37820U 11053A 18089.53824177 .01279251 90211-5 18974-3 0 9990
2 37820 42.7462 210.3658 0008800 350.6458 9.3549 16.333283483736
1 37820U 11053A 18089.78274107 .01688968 90482-5 22274-3 0 9996
2 37820 42.7442 208.7439 0010245 344.1390 16.0283 16.34387332373670
1 37820U 11053A 18090.02708507 .01509296 90500-5 18660-3 0 9992
2 37820 42.7333 207.1177 0007721 347.1312 12.9506 16.35079993373713
1 37820U 11053A 18090.33239452 .01916269 90927-5 20181-3 0 9990
2 37820 42.7393 205.0894 0009533 347.0885 13.3488 16.36467249373764
1 37820U 11053A 18090.51537539 .01668436 91060-5 15733-3 0 9993
2 37820 42.7431 203.8811 0017646 337.7501 22.2668 16.36978516373793
1 37820U 11053A 18090.63734353 .01995214 91302-5 18234-3 0 9994
2 37820 42.7537 203.0502 0007804 350.3894 9.7592 16.37770827373815
1 37820U 11053A 18090.75926316 .01965660 91360-5 17017-3 0 9993
2 37820 42.7468 202.2368 0007442 358.3143 1.7378 16.38245761373833

1 37820U 11053A 18091.00304286 .02715064 91996-5 19001-3 0 9990
2 37820 42.7428 200.6065 0007470 347.8126 12.9725 16.40004788373879
1 37820U 11053A 18091.26319444 +.00000000 +00000+0 +00000+0 0 00005
2 37820 042.7381 198.8688 0006825 342.5456 117.1703 16.41847018000005
1 37820U 11053A 18091.32569444 +.00000000 +00000+0 +00000+0 0 00009
2 37820 042.7351 198.4333 0004504 326.4830 143.2696 16.42540556000003
1 37820U 11053A 18091.42889259 .04822198 92967-5 19530-3 0 9999
2 37820 42.7386 197.7481 0006718 339.4173 21.5137 16.43573928373944
1 37820U 11053A 18091.48949878 .04973923 93030-5 17615-3 0 9996
2 37820 42.7393 197.3406 0006205 338.9313 21.1427 16.44201833373959
1 37820U 11053A 18091.61093320 .05753306 93421-5 14327-3 0 9996
2 37820 42.7382 196.5219 0007050 335.9816 24.1336 16.45676491373975
1 37820U 11053A **18091.67159262** .04847022 93097-5 11856-3 0 9991
2 37820 42.7368 196.1112 0003886 340.8150 19.2351 16.46105415373983

The last TLE set, presented in the table, relates to the time instant of 18091.67159262. This corresponds to the calendar value of the world time (UTC) of 16^h 7^m 5.6^s on April 1, 2018.

3. Results of calculations

For each of two ID updating techniques (OFM and LST), nine versions of the values of a number of measurements n_z were considered: 6, 7… 14. Table 2 presents the basic results of each of problem solutions with various number of measurements with allowance for the last measurement:

- ballistic factor estimate $\hat{S}_b$, m^2/kg;
- reentry time h, m, on April 2, 2018 (UTC);
- residual in the transversal, *delt*, at the last measurement instant, km;
- minimum and maximum *delt* on a fit span, $d\,min$, $d\,max$, km.

Table 2. Basic calculation results

n_z	OFM					LST				
	$\hat{S}_b$	*time*	*delt*	*d min*	*d max*	$\hat{S}_b$	*time*	*delt*	*d min*	*d max*
6	0.00255	1:03	1.4	0.9	2.3	0.00254	1:05	0.9	-1.3	2.1
7	0.00257	1:00	0.6	-4.0	0.7	0.00253	1:03	4.3	-1.9	4.3
8	0.00261	0:51	-1.1	-14.1	-1.1	0.00255	1:18	-10.2	-10.2	2.0
9	0.00268	0:41	-0.6	-2.2	30.9	0.00261	0:31	14.5	-5.8	14.5
10	0.00272	0:22	-0.3	-2.1	58.7	0.00262	0:52	-9.7	-9.7	14.0
11	0.00277	0:20	0.3	-1.5	108	0.00268	0:29	1.1	-12.6	16.9
12	0.00279	0:17	**-1.3**	-3.4	173	0.00270	0:11	**10.3**	-11.0	15.6
13	0.00280	0:13	5.7	2.9	248	0.00270	0:02	15.7	-12.4	15.7
14	0.00282	0:10	0.4	-1.9	310	0.00267	0:05	11.3	-12.9	15.6

It is seen from these results that, for both ID updating techniques, the increase of a number of measurements (the fit span) results in shifting the forecasted reentry

time by 53 (54) minutes in advance. This is caused by the increase of ballistic factor (atmospheric drag) estimates, which is also illustrated by the data of Figure 2.

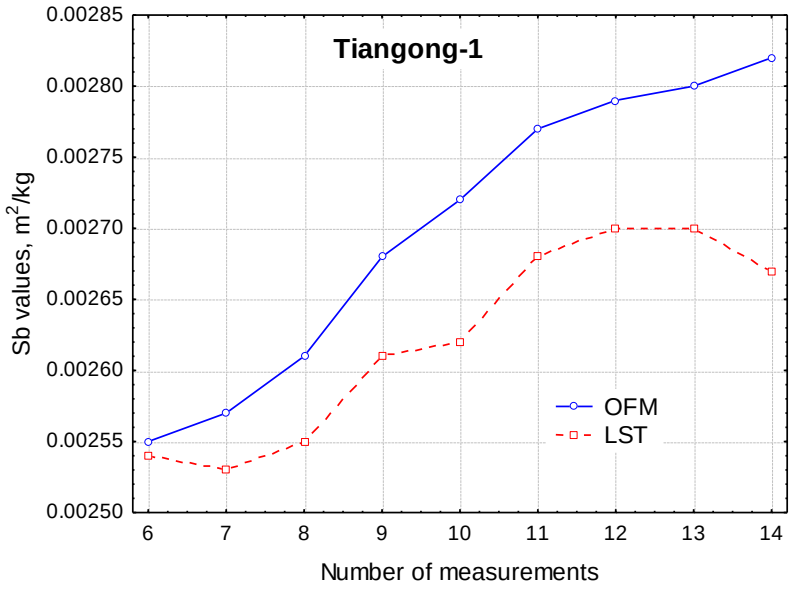

Figure 2. Ballistic factor estimates

Here it is important to pay attention to the fact that, for large fit spans, the LST application does not lead to the acceptable solution: the reference orbit "is inscribed" in the measurements with too large residuals. In addition, in this case the dependence, presented in the figure, is not monotonous. For small values of a number of measurements, the fluctuations of estimates are observed. Such kind of disadvantages are absent in the OFM application results. As the fit span increases, the ballistic factor estimates are stabilized, and residuals remain to be at the former level (of the order of 1 km).

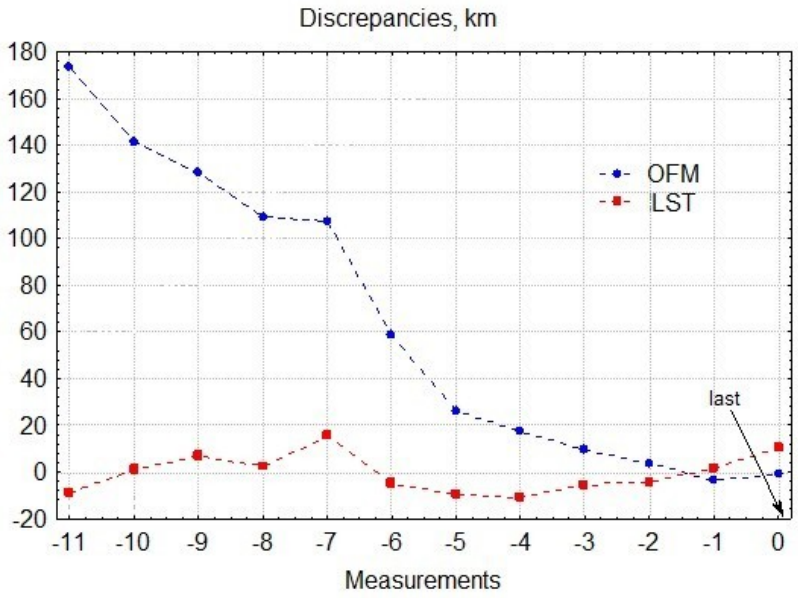

Figure 3. Transversal residuals on the fit span at n_z=12

The principal distinction of the OFM estimates from LST ones consists in the fact that they are based on minimization of errors at the last point of a fit span.

In the LST, the identical weights are assigned to the old and new measurements. As a result, all residuals on a fit span have the same order of magnitude. This situation is illustrated by the data of figure 3 constructed for the version of n_z=12.

When using the OFM, the residual at the last point of a fit span was equal to -1.3 km, and for the LST $delt$=10.3 km; that is, its value occurred to be 8 times greater. In table 2 these estimates are marked by a fat font.

When using the LST, the minimization of errors is reached for versions of n_z=6 and 7, i.e. for the fit spans of 0.45 – 0.60 days. In table 2 a blue background distinguishes these versions. The forecasted reentry time of ≈**1^h 4^m on April 2, 2018** (UTC) corresponds to these versions.

When using the OFM, the most authentic reentry time estimates were obtained for n_z>10, when the ballistic factor estimates were stabilized. The forecasted reentry time in the range from **0^h 10^m to 0^h 20^m on April 2, 2018** (UTC) corresponds to these versions. In table 2 these versions are also distinguished by a blue background. The fit span of 1.5 – 2.0 days corresponds to these versions.

Thus, the reentry time estimates, obtained with using the LST, essentially exceed the corresponding, more authentic reentry time estimates obtained with using the OFM technique.

4. Comparison with published reentry time estimates

a) Table 3. NORAD TIP_msg, site [1].

MSG_ EPOCH	INSERT_ EPOCH	DECAY EPOCH	WINDOW	LAT	LON
2018-04-02 00:59:00	**2018-04-02 01:07:44**	**2018-04-02 00:16:00**	1	-13.6	195.7
2018-04-01 22:53:00	**2018-04-01 23:03:28**	**2018-04-02 00:49:00**	120	-8.9	341.9
2018-04-01 18:18:00	2018-04-01 18:35:42	2018-04-02 00:48:00	120	-9.9	341
2018-04-01 12:18:00	2018-04-01 12:25:23	2018-04-02 00:47:00	180	-13.6	337.1
…	…	…	…	…	…

The first line contains the message that was prepared afterwards, after the satellite reentry (at 00^h 16^m on April 2). It is based on some additional SC measurements and, apparently, is the most authentic estimate of reentry time.

The second line contains the last forecasted reentry time estimate (at 00^h 49^m). The forecast interval up to the reference reentry point is equal to 115 minutes. If we accept the first line's data as the reference (standard) value, then the relative error in a forecast will be:

$$\varepsilon = \text{error/lifetime} = 0.28 = 28\%.$$

b) Aerospace Corporation (site: aerospace.org [6])

"The Tiangong-1 is currently predicted to reenter the Earth's atmosphere around **April 2, 2018 00:30 UTC ± 1.7 hours.**
This prediction was performed by the Aerospace Corporation on April 1, 2018".

This message does not contain any data about the forecast interval.

c) ESA data: Update of April 1, 2018

"With the latest available orbital data and space weather forecasts, the re-entry prediction window is stabilized and shrunk further to the time frame running from the **night of April 1 to the early morning of April 2 (in the UTC time)**".

This message does not contain any particular estimates of reentry time and forecast interval.

d) Table 4. C. Pardini paper [10].

POSTING EPOCH	ORBIT EPOCH	START EPOCH	COIW EPOCH	END EPOCH
YYYY/MM/DD HH:MI:SS	YYYY/MM/DD HH:MI:SS	YYYY/MM/DD HH:MI:SS	YYYY/MM/DD HH:MI:SS	YYYY/MM/DD HH:MI:SS
2018/04/01 08:27:06	2018/04/01 06:19:00	2018/04/01 18:42:40	2018/04/02 00:01:23	2018/04/02 05:20:06
2018/04/01 14:00:49	2018/04/01 11:44:53	2018/04/01 20:50:56	2018/04/02 00:44:59	2018/04/02 04:39:00
2018/04/01 17:47:23	2018/04/01 14:39:45	2018/04/01 21:44:06	2018/04/02 00:45:57	2018/04/02 03:47:50
2018/04/01 18:45:59	2018/04/01 16:07:06	2018/04/01 22:13:26	2018/04/02 00:50:26	2018/04/02 03:27:26

It follows from table's data that the relative error was equal to **6.6 %.**

Figure 4. Map from paper [10]

The paper under consideration contains also the information that, according to the Roscosmos data, the last reentry time estimate was equal to $00^h\ 50^m$. This message did not contain any information on the forecast interval. The resulting data are presented higher on the map.

e) Table 5. V. Yurasov's data, the private message of April 02, 18 00:13.

Orbit epoch (UTC)	GOST-1984	GOST-2004	NRMSIS-00
01.04.18 16:07	02.04.18 00:36	02.04.18 00:54	02.04.18 00:45

The reentry time estimates, presented here, were obtained with using different atmospheric models. They lie within the range from $00^h\ 36^m$ to $00^h\ 54^m$. These values may have relative errors from 3.8 % to 7.2 %.

All reentry time estimates, presented above, lie within the time interval from $00^h\ 30^m$ to $00^h\ 54^m$. They were obtained on the LST application basis and 14–38 minutes exceeded the a posteriori estimate of $00^h\ 16^m$. This fact correlates with the data of table 2 and with the conclusion that, in the considered example, the reentry time estimates, obtained with using the LST, essentially exceeded the corresponding, more authentic estimates.

It was noted above, that the a posteriori reentry time estimate, placed on JSpOC website [1], did not contain the data on the SC altitude at the time instant of $00^h\ 16^m$. To eliminate this uncertainty, it is profitable to use the photo picture of the SC reentry, taken at the Tahiti Island in French Polynesia and published in the Internet on April 2, 2018. This photograph is presented in figure 5.

Figure 5. SC reentry photograph

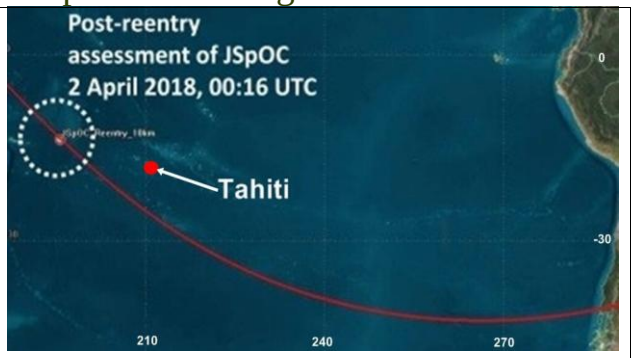

Figure 6. Island position

Figure six shows the fragment of the Pacific Ocean map with the Tahiti Island and a posteriori SC reentry point coordinates. It follows from the data that, at the declared reentry time instant of $00^h\ 16^m$, the SC altitude was rather high, and its descending has proceeded some more minutes.

To estimate the SC altitude at the time instant of $00^h\ 16^m$, it is useful to consider the results of updating and forecasting the SC orbit with using the OFM technique, which were presented in table 2. With optimum algorithm parameters, which are marked in the table by blue color, the forecasted estimates of that altitude were 80 – 95 km. Aerodynamic loadings and heating of SC structure's elements have lead, at these altitudes, to SC destruction, which was just recorded on the photograph at the Tahiti Island. The forecasted estimates of the time, when the SC was located at the declared a posteriori reentry point (with latitude of -13.6º and longitude of 195º), have laid, for the aforementioned calculation versions, within the time interval from $00^h\ 10^m$ to $00^h\ 11^m$. It follows from these estimates, that the time error of forecast was 5 – 6 minutes. With using the initial data at the time instant of $16^h\ 7^m$ on April 1, 2018, the relative forecast error **of $\varepsilon \approx 1$ %** corresponds to this time error.

Thus, application of the OFM technique made it possible, in this case, to decrease the forecast errors several times as compared to the LST application.

Conclusions

1. For the example of the Tiangong-1 SC reentry time determinations, the effect of updating algorithm parameters on the accuracy of results is estimated. The characteristics of accounting for atmospheric perturbances at "weighing" the measurements and the fit span value were considered as the algorithm parameters.
2. In the considered example, the reentry time estimates with using the LST essentially exceeded the corresponding, more authentic estimates obtained with using the OFM.
3. It is shown that, when the random atmospheric perturbances in the OFM technique are taken into account, the accuracy of results grows several times. With using the initial data at the time instant of 16h 7m of on April 1, 2018, relative reentry time error consists of ≈1 of %**.** This output is confirmed also by materials of publications [3, 4, and 5]. The strict mathematical proof of this effect is stated in monograph [5].
4. The application of the OFM technique is a topical and perspective direction of perfecting the ballistic maintenance in the interests of increasing the safety of flights under the conditions of technogenous contamination of the near space. In this case it is necessary to take into account statistical characteristics of perturbances of the other nature: gravitational ones, as well as those associated with the errors of accounting for a light pressure.

Acknowledgement

Authors thank PhD V. Yurasov and PhD C. Pardini for participation in discussion of results of the forecast of the Tiangong-1 SC reentry time.

This research did not receive any specific grant from funding agencies in the public, commercial, or not-for-profit sectors.

References

[1] Two line element (TLE) data, Satellite decay & reentry data. http://www.space-track.org (accessed April 2 2018).

[2] Nazarenko A.I., Markova L.G. Methods of determination and forecasting the AES orbits in the presence of errors in the mathematical description of motion //Applied problems of space ballistics: collection. M.: Nauka, 1973. pp. 36-67.

[3] Nazarenko A.I. Application of the method for optimum filtering of measurements for determination and prediction of spacecraft orbits, Solar System Research , vol. 47 (2013)

[4] Nazarenko A.I., How can we increase the accuracy of determination of spacecraft's lifetime? //Acta Astronautica, 115 (2015), pp. 229-236.

[5] Nazarenko A.I. Stochastic astrodynamics problems. Mathematical methods and solution algorithms. – M: URSS, 2017, 352 p.

[6] https://aerospace.org/cords/reentry-predictions/tiangong-1-reentry/. (accessed April 2 2018).

[7] Nazarenko A.I., Yurasov V.S., Tikhomirova S.V. Determination of the satellite reentry time with allowance for random variations of atmospheric drag. ESOC, Reentry Workshop 2018, Darmstadt.

[8] Earth's Upper Atmosphere. Density Model for Ballistic Support of the Flight of Artificial Earth Satellites. GOST R 25645. Publishing House for the Standards, Moscow, 2004.

[9] Space data, Space weather. https://www.celestrak.com/. (accessed April 2 2018).

[10] Pardini C., Anselmo L. Uncontrolled re-entries of Tiangong-1. 36th IADC Plenary Meeting (Tsukuba, Japan, 5 – 8 June, 2018).